

Transformer-based models and hardware acceleration analysis in autonomous driving: A survey

Juan Zhong, Zheng Liu, Xi Chen

Abstract—Transformer architectures have exhibited promising performance in various autonomous driving applications in recent years. On the other hand, its dedicated hardware acceleration on portable computational platforms has become the next critical step for practical deployment in real autonomous vehicles. This survey paper provides a comprehensive overview, benchmark, and analysis of Transformer-based models specifically tailored for autonomous driving tasks such as lane detection, segmentation, tracking, planning, and decision-making. We review different architectures for organizing Transformer inputs and outputs, such as encoder-decoder and encoder-only structures, and explore their respective advantages and disadvantages. Furthermore, we discuss Transformer-related operators and their hardware acceleration schemes in depth, taking into account key factors such as quantization and runtime. We specifically illustrate the operator level comparison between layers from convolutional neural network, Swin-Transformer, and Transformer with 4D encoder. The paper also highlights the challenges, trends, and current insights in Transformer-based models, addressing their hardware deployment and acceleration issues within the context of long-term autonomous driving applications.

Index Terms—Transformer, Hardware Acceleration, Autonomous Driving, Deep Learning.

I. INTRODUCTION

In recent years, autonomous driving has become a rapidly growing field that aims to assist human drivers with an automated and intelligent system. Successful deployment of autonomous driving techniques is expected to significantly improve safety, efficiency of transportation systems. In the past two decades, a range of data-driven techniques have been developed for autonomous driving, ranging from traditional rule-based approaches [1], [2] to advanced machine learning methods [3]. Traditional approaches for autonomous driving primarily rely on algorithms with analytical expressions and binary encoded traffic

rules to perceive the environment, plan the trajectory, and control the vehicle; see review articles in early to mid 2010s for details, e.g., approaches for urban scenarios [4], motion planning and control [5], [6], and simultaneous localization and mapping (SLAM) tasks [7]. However, these traditional methods often face challenges in handling complex real-world scenarios, such as dynamic objects, occlusions, and uncertain environments. In contrast, deep learning methods [8], particularly deep neural networks (DNNs), have demonstrated remarkable performance in learning complex patterns from data and making predictions. For instance, convolutional neural networks (CNNs) [9], a type of DNNs employ convolutional layers to detect local spatial features and hierarchically combine them to recognize complex patterns, have been widely used in autonomous driving applications. Deep learning methods for different autonomous driving tasks have been reviewed and discussed in previous surveys, including general discussions [3], [10], [11], [12], [13]; models using reinforcement learning [14]; models for object detection [15], trajectory and behavior prediction [16], [17], multi-modal fusion [18], planning and decision making [19], [20], [21], explainability AI [22], and scenario generation [23].

Recently, Transformer architecture [24] has exhibited impressive performance in various autonomous driving tasks over traditional CNN models. As a result, there has been growing interest in the deployment of Transformer models on portable hardware and the development of operator-level acceleration schemes. This survey paper aims to offer a comprehensive and in-depth overview of state-of-the-art research of Transformer-based models, with a particular emphasis on operator-level acceleration techniques for autonomous driving.

Attention mechanism [25] has been introduced to further enhance the performance of CNN-based methods in autonomous driving. The primary idea behind attention mechanisms is to allow the model to weigh different parts of the input based on their relevance to the current context. In the case of sequence-to-sequence models, for example, attention mechanisms

Juan Zhong is with University of the Chinese Academy of Sciences, Beijing, China.

Zheng Liu is with the Department of Engineering, University of Cambridge, Cambridge, UK.

Xi Chen is with the Department of Computer Science, University of Bath, Bath, UK.

Corresponding author: Xi Chen (email: xc841@bath.ac.uk).

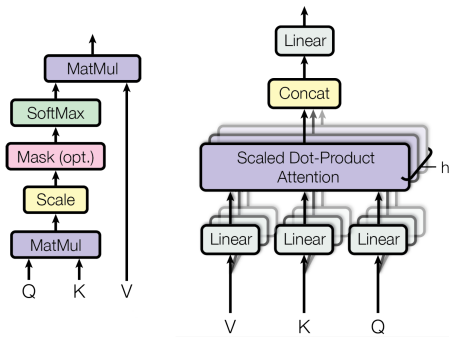


Figure 1. The left panel depicts self-attention (or scaled dot-product attention) and the right panel shows multi-head attention that contains several attention layers, as illustrated in [24].

enable the decoder to focus on specific parts of the source sequence while generating the target sequence. This selective focus allows the model to capture longer-range dependencies and relationships more effectively than traditional recurrent neural networks. As shown in Figure 1, the attention mechanism can be described as a function that computes a weighted sum of a set of input values, also known as "values" (V), based on their compatibility with a given query (Q). The attention mechanism calculates an attention score for each key-query pair using an attention scoring function, and then normalizes these scores using a softmax function to produce attention weights. These weights are used to compute the weighted sum of the values, which represents the output of the attention mechanism. By selectively attending to relevant information, attention mechanisms can improve the efficiency and robustness of learning process.

Transformer architecture [24] was originally developed on attention mechanism for natural language processing (NLP) tasks, but their ability to model long-range dependencies and capture global context has made them attractive for perception tasks in autonomous driving. It aims to process and capture dependencies in input data, which eliminates the need for recurrent or convolutional layers, enabling highly parallelized computation. A typical Transformer consists of an encoder-decoder structure. The encoder is composed of a stack of identical layers, each containing two primary components: a multi-head self-attention mechanism (as shown in Figure 1) and a position-wise feed-forward neural network. The Multi-head attention module enables the model to simultaneously weigh the importance of different parts of the input sequence relative to each other, capturing long-range dependencies. Transformer architecture incorporates positional encoding, which injects information about the relative or absolute position of input elements, as attention mechanism does not inherently capture positional information.

Hardware acceleration of Transformer architec-

ture then become an important area for model implementation in real autonomous driving scenarios. Hardware acceleration on AI chips involves using specialized processors or dedicated hardware units to perform specific operations more efficiently than general-purpose CPUs or GPUs. On the other hand, Transformer operators are the fundamental building blocks of Transformer architectures that perform essential mathematical operations, such as matrix multiplications, attention calculations, and feed-forward neural network computations. The optimization of Transformer operators is crucial to fully harness the capabilities of hardware accelerators and achieve fast, efficient deployment and execution of Transformer-based models. By tailoring these operators to exploit the strengths of AI chips, such as parallelism, lower-precision arithmetic, and specialized functional units, the overall performance of Transformer models can be significantly improved. AI accelerators often employ techniques such as lower-precision arithmetic, data compression, and parallel processing to speed up computations and reduce power consumption.

The rest of this paper is organised as follows. Section II introduces the base Transformer models and various Transformer variants in different autonomous driving tasks. Section III presents different Transformer encoder-decoder structures, operators, and hardware acceleration advances in portable AI devices. Section IV discusses the challenges and trends of Transformer-based deep learning implementations, and followed by a conclusion.

II. TRANSFORMER MODELS AND TASKS

The development history of attention mechanisms and Transformer architectures can be traced through a series of key developments and milestone papers, as shown in Figure 2. Bahdanau et al. [25] first introduced the attention mechanism in the context of neural machine translation, proposing a dynamic alignment method between source and target sequences. This approach overcame the limitations of fixed-length context vectors in earlier sequence-to-sequence models. Luong et al. [26] further refined attention mechanisms by presenting local and global attention, with the former focusing on a smaller source sequence subset and the latter considering all source words for variable-length alignment context computation.

A milestone of this line is by Vaswani et al. [24], who introduced the Transformer architecture for the first time. This innovation led to notable improvements of performance in various NLP tasks. Subsequently, Devlin et al. [27] proposed BERT (Bidirectional Encoder Representations from Transformers), a pre-trained model for bidirectional representations using the Transformer architecture. BERT, when fine-tuned on downstream tasks, achieved unprecedented

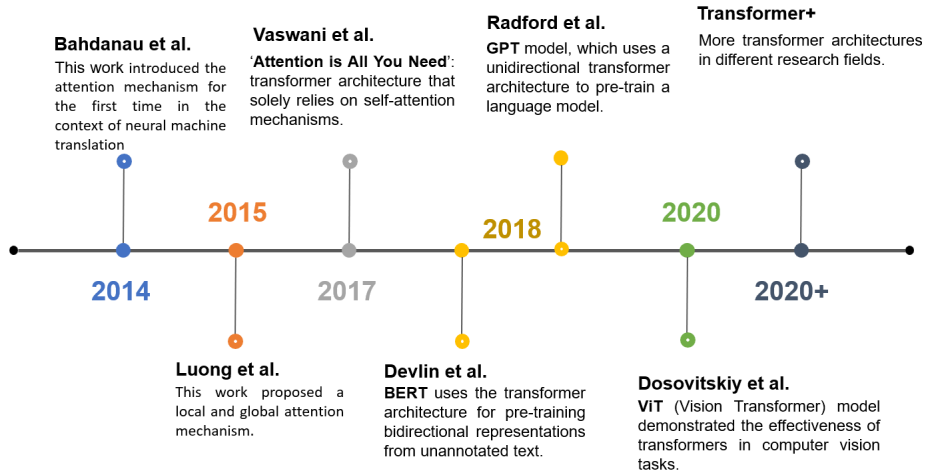


Figure 2. A timeline diagram illustrating the history and key milestones of attention mechanisms and Transformer architectures research.

performance in NLP tasks. In another line of research, Radford et al. [28] presented the GPT (Generative Pre-trained Transformer) model, which employed a unidirectional Transformer architecture for language model pre-training. Fine-tuning GPT on specific tasks yielded substantial performance improvements, with later iterations (GPT-2, GPT-3, and GPT-4) continuing to advance the state-of-the-art. Recently, Dosovitskiy et al. [29] demonstrated the applicability of Transformer architecture to computer vision tasks with the Vision Transformer (ViT) model. By dividing images into non-overlapping patches and using linear embeddings, the authors achieved competitive results compared to traditional CNN models in image classification tasks. ViT is also one of the basic architectures for the follow-up Transformer-based models in image processing tasks.

A. The Base Models for Image Processing

As an pioneer architecture of Transformer-based image processing models, ViT [29] replaced the convolutional layer of a traditional CNN with the self-attention layer. As shown in Figure 3, it divided an image into a sequence of non-overlapping patches, which were then fed into a Transformer encoder to learn a representation of the image. The Transformer encoder consisted of several self-attention layers followed by feed-forward layers. The self-attention mechanism allowed the network to attend to relevant patches in the image while ignoring irrelevant ones. To make the ViT applicable to larger images, the authors introduced a hybrid approach that combined convolutional layers with self-attention layers. The convolutional layers were used to reduce the spatial resolution of the image, while the self-attention layers captured the long-range dependencies between patches.

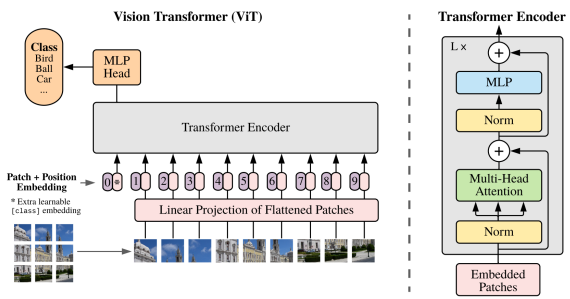


Figure 3. The architecture of ViT, the left panel shows the image division and position embedding process and the right panel presents a standard encoder architecture that contains the multi-head attention layer, as illustrated in [29].

Inspired by ViT, Swin-Transformer [30] introduced a new hierarchical architecture that organized the self-attention mechanism into a multi-level hierarchy, where each level consisted of a group of non-overlapping patches. This approach was motivated by the observation that vision Transformers had limited scalability due to the quadratic complexity of the self-attention mechanism. The main innovation of Swin-Transformer was the use of shifted windows, which allowed patches to attend to their neighbors while avoiding overlapping with adjacent patches. This reduced the number of computations required to compute self-attention and enabled the architecture to scale to larger image sizes. It also introduced a new tokenization scheme that divided an image into non-overlapping patches of fixed size, followed by a recursive grouping of patches into larger "macro-patches" at each level of the hierarchy. This approach helped preserve spatial information and allowed the model to capture both local and global context. Many perception models use Swin-Transformer for backbone to obtain image features, such as BEVFusion [31],

[32] and BEVerse [33].

In autonomous driving applications, Transformer-based architectures have been widely adopted in a variety of sub-tasks, including object detection, lane detection and segmentation, tracking and localization, path planning, and decision-making. Additionally, recent studies have explored the use of Transformer in constructing end-to-end deep learning models for autonomous driving. These models leverage the attention mechanism to further improve their ability to focus on relevant information and perform effectively in complex, real-world driving scenarios. In the rest of this section, we review the Transformer-based models according to their tasks, as presented in Table I. We primarily divide the tasks into three categories: 3D & general perception tasks (including object detection, tracking, and 3D segmentation); 2D & plane tasks (including lane detection, segmentation, and High Definition (HD) map generation); and other tasks (including trajectory prediction, behavior prediction, and end-to-end tasks).

B. 3D & General Perception Tasks

The first category of tasks is 3D and general perception, including object detection, tracking, and 3D segmentation tasks. It is one of the most popular research fields where Transformer-based models are developed in the past few years. This type of task aims to segment, identify, and track objects such as vehicles, pedestrians, and other elements in the environment. Amongst various Transformer-based models, DETR [67] was an early important one that inspired many subsequent works, though it was originally designed for 2D detection. DETR considered object detection as a prediction problem using pre-generated boxes and eliminated traditional anchors. It employed a bipartite matching method based on the Hungarian algorithm to predict one-to-one object sets directly. Variant models such as Deformable DETR [68], had been proposed to enhance the model's convergence speed and address query ambiguity by introducing deformable attention. Building on the DETR architecture, DETR3D [34] applied the Transformer to multiple cameras for 3D object detection in bird's eye view (BEV) space. It first transformed point cloud data (from LiDAR) into a 3D voxel representation and then fed it to a modified DETR architecture that used multi-scale feature fusion to capture both global and local context information. FUTR [69] was also similar to DETR in its architecture but used multi-sensors (images+LiDAR+radar). Multi-modal inputs were fused into a BEV feature and then lifted to achieve 3D BBOX. Building on FUTR, FUTR3D [35] extended 3D object detection to multimodal fusion. It was similar to DETR3D in structure but added a Modality-Agnostic Feature

Sampler (MAFS), capable of handling various sensor configurations and fusing different modalities, including 2D cameras, 3D LiDARs, 3D radars, and 4D imaging radars.

PETR [36], [37] was another recent development that used a position embedding transformation for multi-view 3D object detection. It encoded 3D coordinate position information into image features, producing 3D position-aware features. During inference, the 3D position coordinates could be generated offline and used as an extra input position embedding. CrossDTR [38], which combined the strengths of PETR and DETR3D, created a cross-view and depth-guided framework that achieved comparable accuracy to other methods while offering fast processing times due to fewer decoder layers. BEVFormer [39], [40] took a different approach, employing spatio-temporal Transformer architecture for unified BEV representations to improve performance without relying on multi-modal inputs. It incorporated both spatial and temporal fusion, leveraging historical information for enhanced performance. BEVFormer employed a temporal self-attention module to extract features from historical BEV features for motion target velocity estimation and occluded target detection, and the spatial cross-attention was extended in the vertical direction for columnar queries in the Z direction of BEV. In contrast, UVTR [41] focused on enhancing depth inference by using cross-modal interaction between image and LiDAR inputs, generating separate voxel spaces for each modality in BEV without height compression, and then fusing the multimodal information via knowledge transfer and modal fusion. This approach provided a promising direction for expanding 3D occupancy research.

In the 3D segmentation task, TPVFormer [42] addressed the efficiency issue of Transformer-based methods by transforming the volume to three BEV planes, significantly reducing computational burden while effectively predicting the semantic occupancy of all voxels in space. VoxFormer [43] used 2D images to generate 3D voxel query proposals by depth prediction, and then performed deformable cross-attention query based on these proposal 3D voxel queries from 2D image features. After that, it applied a masked autoencoder to propagate information by self-attention and refined the voxel by an upsample network to generate semantic occupancy results. SurroundOcc [44] performed a 3D BEV feature query from multi-view and multi-scale 2D image features, added 3D convolutions to the Transformer layer, and progressively upsampled the volume features. When multi-level BEV features were produced, its 3D convolution network can combine these features to generate a dense space occupancy.

In the 3D object tracking task, most existing

Table I

SOME TRANSFORMER-BASED MODELS CLASSIFIED BY AUTONOMOUS DRIVING TASKS INCLUDING OBJECT DETECTION AND TRACKING, 3D SEGMENTATION, LANE DETECTION AND SEGMENTATION, HIGH DEFINITION (HD) MAP GENERATION, TRAJECTORY AND BEHAVIOR PREDICTION, AND END-TO-END TASKS. SENSOR TYPE ARE MAINLY (MULTIPLE) RGB CAMERAS AND LiDAR, AND HD MAP INFORMATION IS USED FOR TRAJECTORY PREDICTION TASK. ‘BEV’ INDICATES WHETHER THE MODEL PROVIDES BIRD’S EYE VIEW FEATURES.

Model	Tasks	Data Sources	BEV	Release Year
3D & General Perception				
DETR3D [34]	Object Detection	Camera	N	2021
FUTR3D [35]	Object Detection	Camera, LiDAR	N	2022
PETR [36], [37]	Object Detection	Camera	N	2022
CrossDTR [38]	Object Detection	Camera	Y	2022
BEVFormer [39], [40]	Object Detection	Camera	Y	2022
UVTR [41]	Object Detection	Camera, LiDAR	Y	2022
TPVFormer [42]	3D Segmentation	Camera	Y	2023
VoxFormer [43]	3D Segmentation	Camera	Y	2023
SurroundOCC [44]	3D Segmentation	Camera	Y	2023
MOTR [45]	Object Tracking	Camera	N	2022
MUTR3D [46]	Object Tracking	Camera	N	2022
2D & Plane				
BEVSegFormer [47]	Lane Detection	Camera	Y	2022
PersFormer [48]	Lane Detection	Camera	Y	2022
LSTR [49]	Lane Detection	Camera	N	2020
CurveFormer [50]	Lane Detection	Camera	Y	2023
TiIM [51]	Segmentation	Camera	Y	2022
Panoptic SegFormer [52]	Segmentation	Camera	N	2022
STSU [53]	HD Map Generation	Camera	N	2021
VectorMapNet [54]	HD Map Generation	Camera, LiDAR	N	2022
MapTR [55]	HD Map Generation	Camera	Y	2023
Prediction & Decision Making				
VectorNet [56]	Trajectory/Behavior Prediction	Trajectory and Map info	N	2020
DenseTNT [57]	Trajectory/Behavior Prediction	Trajectory and Map info	N	2021
mmTransformer [58]	Trajectory/Behavior Prediction	Trajectory and Map info	N	2021
Agentformer [59]	Trajectory/Behavior Prediction	Camera	N	2021
Wayformer [60]	Trajectory/Behavior Prediction	Trajectory and Map info	N	2022
TransFuser [61]	End-to-End	Camera, LiDAR	Y	2022
NEAT [62]	End-to-End	Camera	Y	2021
InterFuser [63]	End-to-End	Camera, LiDAR	Y	2022
MMFN [64]	End-to-End	Camera, LiDAR, Radar, HD Map	Y	2022
STP3 [65]	End-to-End	Camera	Y	2022
UniAD [66]	End-to-End	Camera	Y	2023

methods rely on heuristic strategies that uses spatial and appearance similarities. However, they often fail to effectively model temporal information. Recent Transformer-based models aims to mitigate the issue. For example, MOTR [45] extended the DETR model and built a multiple-object tracking (MOT) framework. It introduced a ”track query” to model tracked instances throughout a video, designed to exploit temporal variations in video sequences and implicitly learn long-term temporal changes in targets, avoiding the need for explicit heuristic strategies. Unlike traditional methods that relied on motion-based and appearance-based similarity heuristics and post-processing techniques, MOTR handled object tracking without requiring track NMS or IoU matching. MUTR3D [46] simultaneously performed detection and tracking by employing cross-camera and cross-frame object association based on spatial and appearance similarities. This approach utilized a 3D track query to directly model an object’s 3D states and appearance features over time and across multiple cameras. During each frame, the 3D track query sampled features from all visible cameras and learnt

to initiate, track, or terminate a track.

Transformer-based approaches have made impressive progresses in 3D and general perception tasks, emphasizing the potential of developing specialised attention mechanism for a wider range of perception tasks in more complex and realistic autonomous driving scenarios.

C. 2D & Plane Tasks

In contrast to the 3D task category, we classify a second task category as 2D and plane tasks where the models primarily address tasks such as lane detection, segmentation, and HD map generation.

For the lane detection task, we further divided the models into two groups. The first group of models generate BEV features followed by CNN semantic segmentation and detection heads. For example, BEVSegFormer [47] used a cross-attention mechanism to query multi-view 2D image features. A semantic decoder was added after the Transformer to decode the query into BEV road semantic segmentation results. PersFormer [48] extracted image

features using a CNN and split them into two paths. The first path connected to a CNN-based 2D lane detection head, while the second path used an inverse perspective mapping (IPM) method to transform perspective view (PV) view features to BEV view features, connected to the Transformer network for BEV feature querying and enhancement. The second group of models directly queried and generated road structures using various representations such as polynomials, key points, vectors, and polylines. For instance, LSTR [49] approximated flat single-lane road markings with second- or third-order polynomials. A Transformer query was used to update the parameters of the polynomial, and the Hungarian matching loss optimized the path-related regression loss. LSTR adopted a lightweight Transformer architecture for more efficient querying. CurveFormer [50] accelerated inference speed by directly generating lane lines from 2D images without the need for feature view transformations. It employed a Transformer decoder, using curve queries to transform the 3D lane detection formula into a curve propagation problem, with a curve intersection attention module to calculate the similarity between curve queries and image features.

In addition to lane detection, Transformer architecture is also utilized in segmentation tasks. For example, TliM [51] presented a sequence-to-sequence model for instantaneous mapping, which converted images and videos into overhead maps or BEV representations. By assuming a one-to-one correspondence between vertical scan lines in images and rays in overhead maps, TliM was claimed as a data-efficient and spatially-aware method. Panoptic SegFormer [52] proposed a framework for panoptic segmentation that combined semantic and instance segmentation. It presented supervised mask decoder and a query decoupling strategy to perform efficient segmentation.

For the HD map generation task, STSU [53] represented lanes as directed graphs in BEV coordinates and learned Bezier control points and graph connectivity based on simple multilayer perceptron (MLP). It adopted a DETR type query method to convert front-view camera images into BEV road structures. VectorMapNet [54] was the first Transformer network to achieve end-to-end vectorization for high-precision maps [70], modeling geometric shapes using sparse polyline primitives from a BEV view. It employed a two-stage pipeline consisting of set prediction for detecting rough key points and sequence generation for predicting the next point of the map element. MapTR [55] developed a framework for online vectorized high-precision map generation that modeled map elements as point sets with a set of equivalent envelopes. It introduced a hierarchical query embedding scheme to flexibly encode instance-level and point-level information and learned structured

bipartite matching of map elements. These models have been shown to effectively merge multi-view features into a unified BEV view, facilitating end-to-end online high-precision map construction, which is crucial for other downstream tasks.

D. Prediction and Decision Making

In addition to the 2D/3D perception tasks, Transformer architecture is also adopted in other tasks such as prediction, planning, and decision-making. Furthermore, recent studies have explored the use of Transformers in constructing end-to-end DNN models for the whole autonomous driving pipeline, which aim to unify perception, planning, and control into a single integrated system.

For trajectory or behaviour prediction, there exists practical challenges for feature extraction by the standard CNN model, especially its limited capacity to model long-range interactions. Transformer-based models are then developed to address this issue. VectorNet [56] was developed to transform these geometric shapes (from road markings or vehicle trajectories) into vector format inputs. It introduced a hierarchical graph neural network that encoded HD maps and agent trajectories using vector representations, and also exploited spatial locality of individual road components and modeled their interactions. TNT [78] defined vehicle modes based on the endpoint of each trajectory and simplified trajectory prediction by converting it into an endpoint prediction problem. However, as an anchor-based technique, TNT required heuristic anchor definitions before predicting the endpoint. DenseTNT [57] was developed to overcome this limitation by directly predicting the probability distribution of the endpoint, enabling anchor-free prediction. mmTransformer [58] proposed a stacked Transformer architecture to model multi-modality at the feature level with a set of fixed independent proposals. A region-based training strategy was then developed to induce the multi-modality of the generated proposals. This strategy reduced complexity of motion prediction while ensuring multimodal behavior outputs. AgentFormer [59] allowed an agent's state at a specific time to directly impact another agent's future state, eliminating the need for intermediate features encoded in a single dimension. This approach enabled the simultaneous learning of temporal information and interaction relationships. It also ensured an agent's current relationship was reflected through relationships at various times, mitigating the loss of time and agent information that typically occurred with equal input element status in traditional Transformer attention mechanisms. For more complicated situations, where the inputs contain both static and dynamic data (e.g., road geometry, lane connectivity, traffic light

Table II

BENCHMARK PERFORMANCE OF TRANSFORMER MODELS ON A STANDARD NVIDIA GTX3090 GPU. ‘BACKBONE’ DESCRIBES THE BACKBONE ARCHITECTURE OF EACH MODEL AND ‘PARAM.’ REPRESENTS THE SIZE OF MODEL PARAMETERS. ‘GFLOPS’ STANDS FOR GIGA FLOATING POINT OPERATIONS PER SECOND, ‘FPS’ IS FRAMES PER SECOND, AND ‘mAP’ REPRESENTS MEAN AVERAGE PRECISION OF THE MODEL. THE LAST COLUMN INDICATE THE BENCHMARK DATASET USED FOR EACH MODEL.

Task	Model	Backbone	Input Size	Param.	GFLOPs	FPS	mAP	Dataset
Base Model	ViT [29]	-	224x224	85.8M	16.86	14.0	0.81	ImageNet [71]
	Swin-T [30]	-	224x224	86.8M	15.14	27	0.81	ImageNet
Object Detection	DETR [67]	ResNet50	800x800	42.22M	73.4	9	0.385	Coco [72]
	DETR3D [34]	ResNet101	6x1600x900	51.3M	1016.8	2.0	0.349	Nuscenes [73]
	FUTR3D [35]	ResNet101	6x1600x900	47.7M	1023	1.9	0.346	Nuscenes
	BEVFormer [39]	ResNet101	6x1600x900	68.7M	1303.5	2.3	0.375	Nuscenes
	PETR [36]	ResNet101	6x1408x512	59.2M	504.6	5.3	0.357	Nuscenes
	PETR	ResNet50	6x1408x512	35.8M	290.0	10.4	0.341	Nuscenes
	CrossDTR [38]	ResNet101	6x1408x512	53.3M	483.9	5.8	0.370	Nuscenes
CrossDTR	ResNet50	6x1408x512	31.8M	268.1	10.6	0.326	Nuscenes	
Lane Detection	LSTR [49]	ResNet18	1x640x360	765.8K	1.15	89.6	0.962	TuSimple [74]
	Persformer [48]	EfficientNet	1x480x360	47.7M	142.8	24.03	0.505	OpenLane [75]
HD Map	MapTR [55]	ResNet50	6x800x450	36.2M	-	16.6	0.762	Nuscenes
	MapTR	ResNet18	6x320x180	15.4M	-	34	0.642	Nuscenes
Prediction	DenseTNT [57]	-	1x296x128	617.8K	39.23	7.41	0.328	Argoverse [76]
End-to-End	Transfuser [61]	RegNetY	256x256 (LiDAR)	165.6M	33.8	59.6	61.18	CARLA [77]
	Interfuser [63]	RegNetY	704x160 (RGB)					
		ResNet18	224x224 (LiDAR)	82.8M	46.5	38.2	71.18	CARLA
		ResNet50	800x600 (RGB)					

etc.), it is challenging for a standard Transformer to model extensive multi-dimensional sequences due to its quadratic reliance on input sequence length for self-attention and costly position-wise feed-forward networks. WayFormer [60] mitigated this issue by analyzing pre-fusion, post-fusion, and hierarchical fusion for inputs and maintained a balance between efficiency and quality. The method avoided the complex process of designing modality-specific modules, making it easier to scale and extend the model.

Finally, the end-to-end models are broadly classified as a planning and decision making task since the final goal of an end-to-end task is to output decision signal. Several work emerged in the past few years, for example, TransFuser [61] used multiple Transformer modules for data processing, intermediate data fusion and feature map generation. Data fusion was applied at multiple resolutions (64x64, 32x32, 16x16, and 8x8) throughout the feature extractor, resulting in a 512-dimensional feature vector output from both the image and LiDAR BEV streams, which were then combined via element-wise summation. The approach considered sensing regions within 32m in front of the ego-vehicle and 16m to each side, thereby encompassing a BEV grid of 32m x 32m. The grid was divided into blocks of 0.125m x 0.125m, resulting in a resolution of 256 x 256 pixels. NEAT [62] proposed a representation for efficient reasoning of semantic, spatial, and temporal structure of scenes. It constructed a continuous function that mapped locations in BEV scene coordinates to waypoints and semantics, using intermediate attention maps to iteratively compress high-dimensional 2D image features into a compact representation. Based on the TransFuser architecture, InterFuser [63] proposed a

one-stage architecture to fuse information from multi-modal multi-view sensors and achieved better performance. This framework enhanced safety of the end-to-end model by developing a safety control filter to constrain Transformer output actions. Model’s safety-insensitive outputs consist of a 10-waypoint path, while the safety-sensitive outputs include traffic rule information and an object density map with seven features for objects such as vehicles, pedestrians, and bicycles. These outputs are produced by fusing multi-view image inputs and LiDAR point cloud data, which covers a region extending 28 meters in front of the ego-vehicle and 14 meters to its sides. The analyzed area measures 20m x 20m and is divided into 1m x 1m grids. In addition to Camera and LiDAR signals, MMFN [64] made use of vectorized HD maps and radar in the end-to-end task. It explored different representations on the HD map as the network input and proposed a framework to fuse the four types of data. Another work termed STP3 [65] proposed an egocentric aligned accumulation scheme, which converted 2D to 3D and aligned the target features. Its prediction module integrated information from both the obstacle at time t , and the obstacle position at time $t - n$. Unlike the works mentioned above that primarily designed for end-to-end tasks, UniAD [66] presented a planning-oriented framework. The paper argued that previous works failed to consider certain components necessary for planning, and the new design could properly organize preceding tasks to facilitate planning.

In summary, recent Transformer models have been designed to integrate various tasks, aiming for a more end-to-end structure. It is anticipated that future research on end-to-end Transformer models is more

likely to quickly grow, focusing their efficiency and versatility.

E. Benchmark of Transformer Models

We benchmark major Transformer-based models on an NVIDIA GPU 3090 considering indicators such as input size, runtime, accuracy, and datasets. As shown in Table II, for 3D object detection task using Nuscenes dataset [73], both DETR3D and FUTR3D exhibit comparable performance due to their similar structures. BEVFormer outperforms DETR3D by generating BEV features and querying 3D objects from these features. PETR and CrossDTR transform 2D features into 3D features using CNN networks, accelerating the query process and yielding better performance than DETR3D. ResNet101's higher precision compared to ResNet50 can be attributed to its deformable convolution mechanism and increased convolution depth, although at the cost of slower runtime speed [79]. On the other hand, Transformer-based road element detection research exhibits greater variation, with different models and evaluation criteria for tasks such as 2D lane (TuSimple), 3D lane (OpenLane), and local map (Nuscenes). Lane and local map Transformer queries are faster than object detection due to fewer key-point queries and smaller CNN backbones that utilize shallower layer features. As shown at the bottom of the Table, end-to-end Transformer is an emerging field of research. However, it mainly relies on simulated data in unrealistic simulator platforms such as CARLA [77], which limits its applicability to real-world scenarios and practical implementations.

III. TRANSFORMER STRUCTURE, OPERATOR, AND HARDWARE ACCELERATION

This section focuses on Transformer components, operators, and hardware acceleration analysis. We first analyze the encoder-decoder structure, emphasizing its role in processing input data and generating output predictions. Key components, including layer normalization, matrix multiplication, and softmax, are discussed. We then explore methods for enhancing the computational efficiency of Transformer models, detailing hardware acceleration techniques for fixed-point arithmetic applied to operators such as softmax, layer normalization, activation functions, and matrix multiplication.

A. Encoder-Decoder Designs

Despite the state-of-the-art performance achieved by Transformer models in autonomous driving applications, their considerable storage and computational overhead pose challenges for deployment and efficient inference on portable or edge devices.

The Transformer model for perception tasks primarily utilizes BEV features, with the Encoder responsible for generating these features (Figure 4(b) and (d)). The Encoder expands the BEV features into $H \times W$ matrix with a length of Channel, serving as the Query in Transformer. These features are derived from the 2D features of multi-view cameras using the camera extrinsic matrix. To retain the 2D spatial information, position embedding is added to the Query, which then serves as input to the Encoder (Figure 4(b)). For faster convergence, the Encoder iterates the previous BEV features with the current Query as input for self-attention. Additionally, the vehicle's position pose information is matched at the pixel level for front and back frames (Figure 4(d)).

In perception tasks, the CNN head is replaced by a Transformer block to generate 3D bounding boxes for obstacles, as well as 2D/3D lane lines and local maps using queries (Figure 4(a), (c), (e), (f)). There are two types of queries for 3D obstacle perception tasks: explicit and implicit. The explicit query relies on the BEV features (Figure 4(e)), while the implicit query directly uses the 2D feature from the multi-view camera (Figure 4(a)). Implicit queries reduce the computational requirements of the Encoder. To further decrease the computational load on the Transformer, the converted BEV feature can be queried after transformation from the camera perspective view to 2D/3D BEV using a CNN architecture (Figure 4(c)). Lane and local map tasks primarily utilize the BEV feature for queries, with physical keypoints of lanes and local maps as query objects, and their features (xyz, attributes) as vectors. Road information queries necessitate a higher degree of grid refinement for BEV features compared to obstacle tasks; however, the distance range required for BEV features is lower. Vehicles are concerned with both surrounding road information (typically 60m x 30m) and obstacles (typically 100m x 100m), as well as distant obstacles in high-speed scenarios. Since road information is static, it can be constructed using front-view cameras with historical information, while dynamic obstacles require the involvement of side cameras. Consequently, the Transformer's cross-attention mechanism can be flexibly designed and optimized for different applications, based on these requirements.

B. Operators in Different Architectures

In the previous section, the general framework of the Transformer's encoder and decoder for perception tasks was analyzed, with the most complex component being the encoder structure (Figure 4(d)). This structure, employed in BEVformer, spatially and temporally fuses multi-view camera and historical information, respectively, making it a intricate open-

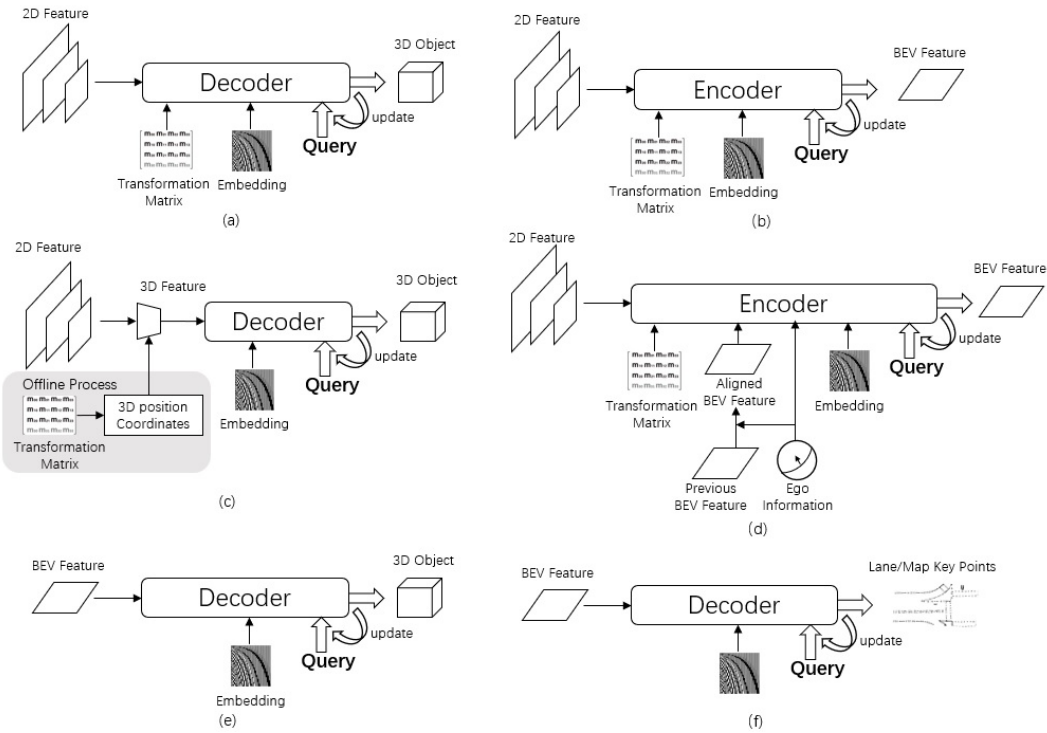


Figure 4. Transformer inputs and outputs in different encoder and decode structures: (a) Object query from 2D image features; (b) BEV feature map query from 2D image features; (c) Object query from 3D features generated by 2D image features using camera extrinsic matrix; (d) BEV feature map query from previous features by ego information and 2D image features; (e) Object query from BEV features; (f) Road elements query from BEV features.

source Transformer for autonomous driving applications. We now disassemble the encoder in terms of operators to obtain the detailed model for subsequent hardware acceleration reference.

In this section, we specifically compares layers of three primary architectures at operator level: ResNet [80], Swin-Transformer, and the encoder of BEVFormer. As shown in Figure 5(a), ResNet features a basic unit called the Bottle Neck and consists of multiple stages containing similar Bottle Neck networks. These networks include 3x3 convolutions, 1x1 convolutions, Batch Normalization (BN), and activation functions (ReLU, rectified linear unit), demanding modest computational parallelism and on-chip memory. In autonomous driving tasks, ResNet is typically utilized for 2D camera image feature extraction, serving as a backbone network.

Figure 5(b) shows the Swin-Transformer that comprise multiple stage units, including data rearrangement, Layer Normalization (LN), Matrix Multiply (32x32), Softmax, Fully Connected (FC) layers, and activation functions (GELU, Gaussian Error Linear Unit). Compared to ResNet, the Swin-Transformer exhibits a greater diversity of operators and larger matrix multiplication dimensions. Softmax and FC layers, which usually appear as the final layer in CNN networks, are found in every Swin-Transformer Stage, necessitating acceleration within the unit. Al-

though Swin-Transformer can replace ResNet as a backbone component in autonomous driving tasks, CNN networks remain mainstream in deployed products due to the trade-off between gains and acceleration performance. As a fundamental Transformer network, the Swin-Transformer serves as an initial reference for hardware acceleration by various NPU manufacturers, achieving performance levels of 3 FPS/TOPS or higher.

The main challenge in accelerating Transformers for autonomous driving stems from the encoder and decoder models that contain both self-attention and cross-attention modules. Cross-attention, which transforms vectors from one space (PV) to another (BEV), is more complex than the self-attention. As shown in Figure 7, we take BEVFormer’s encoder as another example, which comprises temporal self-attention, spatial cross-attention, LN, and FFN. The LN and FFN structures resemble those of the Swin-Transformer, but with larger input and output feature dimensions, necessitating greater computational power. Deformable-attention in the temporal self-attention module employs learnable attention pixel addresses, requiring data fetching from corresponding positions in the data cache. This process involves large matrix multiplication (512*128) and manipulation for extensive matrices, rendering it more complex than the Swin-Transformer’s self-attention.

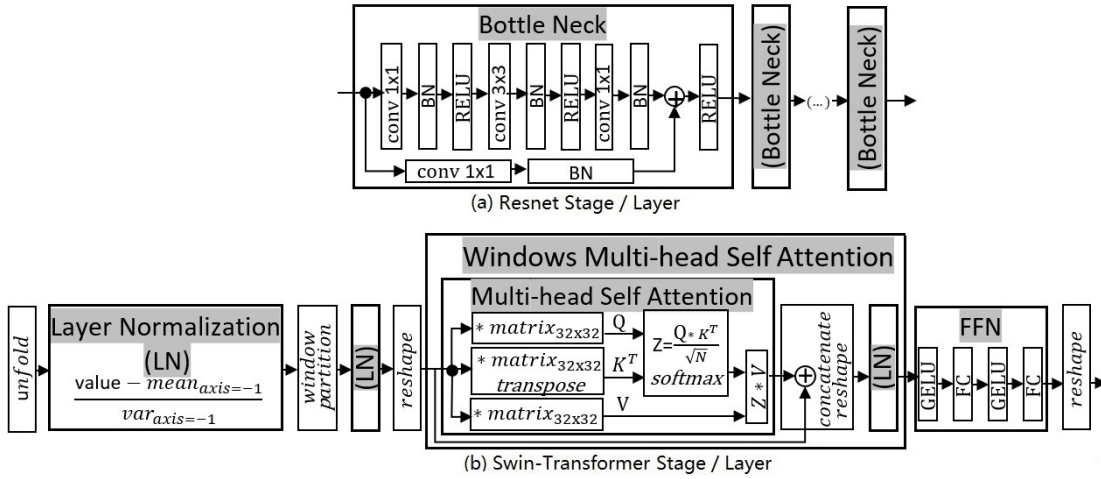


Figure 5. Layers in ResNet and Swin-Transformer: (a) The ResNet basic unit, known as the “bottleneck,” comprises 1x1 and 3x3 convolutions, batch normalization (BN), and the ReLU activation function. (b) The first stage of the Swin-Transformer consists of layer normalization, multi-head self-attention, and a feed-forward network (FFN). The self-attention mechanism involves matrix multiplication, softmax, transposition, concatenation, and reshaping operations. The FFN includes a fully connected layer and the GELU activation function. Furthermore, the Swin-Transformer involves additional data reorganization operations such as window partitioning and unfolding, making its structure more complex than that of ResNet.

The temporal self-attention module fuses current and historical BEV features using the self-attention mechanism. The spatial cross-attention module shares similarities with temporal one, but retrieving attention pixel addresses for multi-camera and multi-scale features proves more intricate due to numerous data manipulation operations and larger matrix multiplication dimensions (512*256). The model complexity for perception tasks in autonomous driving is significantly higher than that of the Swin-Transformer and traditional CNN backbone networks, resulting in increased demands for operator acceleration and on-chip storage.

Additionally, in Figure 6 we show an example of operator list for implementing a Transformer architecture onto portable hardware. The whole process is divided into 26 operator-specific steps, with various indicators reported for each step, such as the operation type, number of multi-heads, repetition counts, and operator time in microseconds. One sees that item 2-5 (Q, K, V and attention matrix calculation), 11 (attention solving head-matrix calculation), 21 (Solving FFN-matrix calculation), and 23 (linear matrix calculation) occupy the majority of the operation counts.

C. Operator Acceleration Analysis

The Transformer architecture contains a large amount of matrix multiply operators and corresponding data carrying operators, Softmax operator, activation function, and LN operator. Quantizing both weights and inputs can speed up inference by tuning floating-point operations into integer [81], [82], [83].

We have designed the hardware acceleration of these operators in a fixed point.

1) *Softmax*: The softmax function is widely used in deep learning, often appearing in the output layer. Previous work [84], [85], [86] has investigated hardware acceleration for softmax in DNN applications, while some studies have also explored quantization and acceleration of softmax based on vision Transformers [87], [81]. Given $\mathbf{x} = [x_0, x_1, \dots, x_{N-1}]$, the standard softmax activation can be defined as

$$\text{softmax}(\mathbf{x}) = \left[\frac{e^{x_0}}{\sum_{j=0}^{N-1} e^{x_j}}, \frac{e^{x_1}}{\sum_{j=0}^{N-1} e^{x_j}}, \dots, \frac{e^{x_{N-1}}}{\sum_{j=0}^{N-1} e^{x_j}} \right] \quad (1)$$

To prevent polynomial summation overflow in the denominator, it is required to perform numerically stable processing during hardware acceleration, we define $m = \max(x)$ and perform a low-precision, replacing the bottom e with 2 to obtain

$$\text{softmax}(\mathbf{x}) = \left[\frac{2^{x_0-m}}{\sum_{j=0}^{N-1} 2^{x_j-m}}, \frac{2^{x_1-m}}{\sum_{j=0}^{N-1} 2^{x_j-m}}, \dots, \frac{2^{x_{N-1}-m}}{\sum_{j=0}^{N-1} 2^{x_j-m}} \right] \quad (2)$$

During the online operation, we focus on parallelization and storage optimization and observed that the time complexity of the entire process is $3O(n)$, and the space complexity is $S(N+1)$. The method requires three loops and stored $N+1$ intermediate results. To optimize the process further, the global maximum is replaced with the local maximum, enabling the calculation to be completed in two loops [87]. This reduces the time complexity to $2O(n)$ and decreased the storage of intermediate results.

In the fixed-point test, the input utilizes signed S6.9 and S5.2, while the output employs unsigned

No.	Calculation Step	Operation Type	Multi_head Quantity	Encoder Internal Repetition Count	Decoder Internal Repetition Count	Total Operation Count	Operator Time (us)	Parameter Category	Size Setting
1	Calculate input I+P	Addition	1	1	1	3686400	9	N	1200
2	Matric calculation Q	MAC	1	1	2	7549747200	1152	C	1024
3	Matric calculation K	MAC	1	1	2	7549747200	1152	h	4
4	Matric calculation V	MAC	1	1	2	7549747200	1152	N_encode	0
5	Attention Matric calculation -A	MAC	4	1	2	8847360000	1350	N_decode	3
6	Attention A/sqrt(N)	Floating-point multiplication	4	1	2	34560000	84.375	C/h	256
7	Attention solving softmax(Aij)-eij	Exponent	4	1	2	34560000	84.375		
8	Attention solving softmax(Aij)-sum	Floating-point addition	4	1	2	34560000	84.375	Operation Type Statistics	
9	Attention solving softmax(Aij)-1/sum	Floating-point division	4	1	2	24	0.06	MAC	7
10	Attention solving softmax(Aij)-e * 1/sum	Floating-point multiplication	4	1	2	34560000	84.375	Multiplication	0
11	Attention solving head-matrix calculation Oi	MAC	4	1	2	8847360000	1350	Addition	1
12	Solving ADD and NORM-O+I	Floating-point addition	1	2	3	11059200	27	Subtraction	2
13	Solving ADD and NORM-calculating average sum	Floating-point addition	1	2	3	11059200	27	Division	0
14	Solving ADD and NORM-calculatnig average sum/nc	Floating-point multiplication	1	2	3	9	0.0225	Exponent	2
15	Solving ADD and NORM-calculating variance	Subtraction	1	2	3	11059200	27	Floating-point addition	5
16	Solving ADD and NORM-calculating variance	Floating-point multiplication	1	2	3	11059200	27	Floating-point multiplication	5
17	Solving ADD and NORM-calculating variance	Floating-point addition	1	2	3	11059200	27	Floating-point division	2
18	Solving ADD and NORM-calculating variance	Square root	1	2	3	9	0.0225	Square root	1
19	Solving ADD and NORM-solving norm	Subtraction	1	2	3	11059200	27	Activation LUT	1
20	Solving ADD and NORM-solving norm	Floating-point multiplication	1	2	3	11059200	27		
21	Solving FFN-matrix calculation O	MAC	1	1	1	3774873600	576	CPU Clock Speed (MHZ)	
22	Solving FFN-relu(O)	Activation LUT	1	1	1	3686400	9	400	
23	linear-matrix calculation O	MAC	-	-	-	1258291200	192		
24	Output solving softmax(Aij)-eij	Exponent	-	-	-	1228800	2.56	Total Calculation Time (ms)	
25	Output solving softmax(Aij)-sum	Floating-point addition	-	-	-	1227600	2.5575	7.064935	
26	Output solving softmax(Aij)-e/sum	Floating-point division	-	-	-	1228800	2.56		
								Total Number of Calculations	
								45603838842	

Figure 6. A table lists primary operators for deploying an example Transformer model onto the portable hardware. Parameter Category: N represents input sequence length, also known as token length, which represents the feature map’s HxW in images, C represents channel dimension, h describes the Multi-head is split into h heads, N_encode indicates the number of times the Encode is repeated, N_decode indicates the number of times the Decode is repeated. We divide the process into 26 operator-wise steps and report indicators including the type of operation, multi-head quantity, repetition counts, and operator time in microsecond (us). The smaller tables on the right present the summary of the main table.

U1.15 and U1.7. The intermediate accumulated result, $\sum_{j=0}^{N-1} 2^{(x_j-M)}$, uses U10.10. The test outcomes are presented in Table III. One sees that the accuracy for 16-bit input and output is approximately 1%. However, the accuracy for 8-bit input is significantly lower, and 8-bit output results in substantial quantization errors. Consequently, the authors recommend using 16-bit quantization for input and output to ensure accuracy in hardware acceleration of the Softmax function.

2) *Layer Normalization*: Layer Normalization (LN) [88], [89] differs from Batch Normalization in that it normalizes across channels rather than batches, addressing the significant amount of computation in the channel direction of Transformer models. This

normalization technique effectively mitigates gradient vanishing and exploding issues during the training of Transformer models. In addition, The Layer Normalization involves operations like division, square and square root, the replacement of layer normalization as well as the attention in the Integer Transformer supports fully INT8 inference [90]. The original calculation formula for Layer Normalization [91] is:

$$\bar{x} = \frac{x - \mu(x)}{\sigma(x)} \cdot \gamma + \beta \quad (3)$$

where:

$$\mu = \frac{1}{C} \sum_{i=1}^C x_i \quad (4)$$

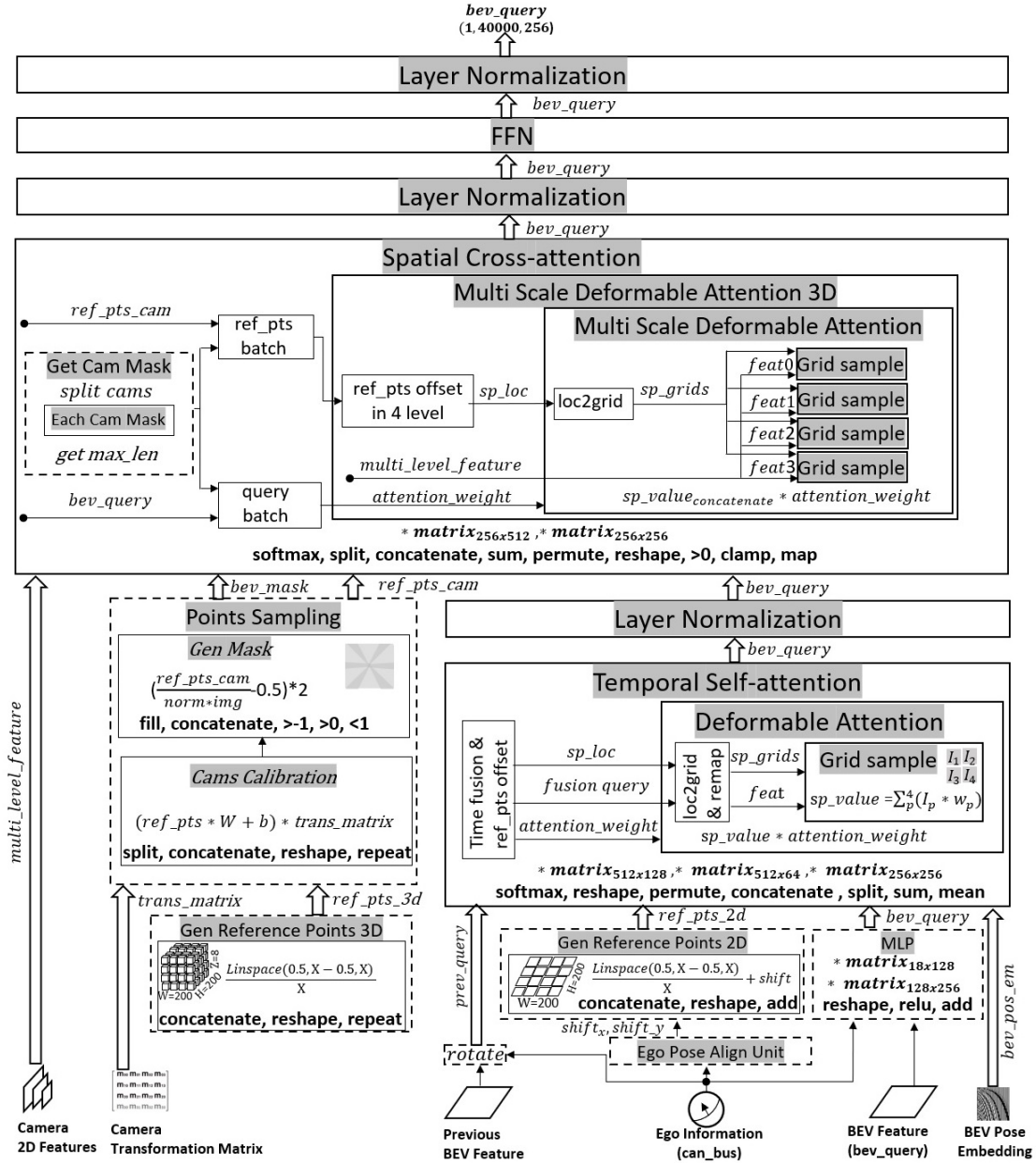


Figure 7. Transformer 4D Encoder Structure: BEVformer encoder structure "encoder layer", the same as Swin-Transformer, BEVformer encoder has Layer Normalization, FFN. There are two complex attention mechanisms, Temporal Self-attention and Spatial Cross-attention. Temporal Self-Attention performs deformable attention on bev query initialized by the previous BEV feature and current BEV feature with ego information calibration. Different to Swin-Transformer, there is a grid sample that will gather features from related positions and these positions are learnable from features and matrix transformation. Spatial cross-attention will help BEV feature query from 2D surround camera features, it also uses deformable attention mechanism. This query is a multi-level and multi-cameras query, so there are 2 modules additional, one is Camera mask module which will generate each camera mask in BEV space, one is multi-level offset module which will get reference point offset in 4 levels. Beside Layer Normalization, activation, softmax, matrix multiply, there are a lot of data reorganization process in BEVFormre encoder such as reshape, split, concatenate, permute etc. BEVformer structure is more complex than Swin-Transformer and acceleration will be much more difficult.

Table III
FIXED-POINT WITH DIFFERENT QUANTIZATION FOR SOFTMAX,
LAYER NORMALIZATION(LN) AND GELU OPERATORS, WITH
8-BIT AND 16-BIT BIT WIDTH I/O COMBINATIONS,
RESPECTIVELY. ANALYSIS THE MEAN AND MAX ERROR
COMPARED TO 32-BIT FP32 I/O RESULT.

Operator	Bit width I/O	Mean Err. %	Max Err. %
Softmax	S6.9/U1.15	0.63	1.56
	S5.2/U1.15	4.44	9.56
	S6.9/U1.7	99.69	100
LN	Case1 (S7&U8/S8.7)	0.49	1.75
	Case2 (S7&U8/S8.7)	0.58	6.12
GELU	S6.9/S5.10	0.82	-
	S3.4/S5.10	5.73	-
	S6.9/S3.4	28	-

$$\sigma = \sqrt{\frac{1}{C} \sum_{i=1}^C (x_i - u)^2}. \quad (5)$$

According to the quantization formula:

$$x = (X_Q - zp) \cdot S \quad (6)$$

where X_Q is the quantized fixed-point activation value, S is the scale factor, zp is the input zero point. β and γ are the input parameters (floating-point numbers).

After derivations, the Layer Normalization calculation formula can be expressed as:

$$\bar{x} = \frac{1}{\sigma(X_Q)} \cdot (\gamma \cdot X_Q - \gamma \cdot \mu(X_Q) + \beta \cdot \sigma(X_Q)) \quad (7)$$

We designed and tested a fixed-point hardware accelerator for the given formula. The tests utilized 8-bit $U8$ and $S7$ inputs, 16-bit $S8.7$ outputs, and intermediate results with varying quantization precisions. The mean value employed $S8.7$, while the standard deviation utilized $U8.6$. We evaluated the performance on two distinct test data sets, referred to as case1 and case2, and reported the results in Table III (rows four to five). The test outcomes revealed comparable output results for $S7$ and $U8$. The maximum error percentage predominantly occurred at the sequence's smallest value. Although the absolute error value remained small, the error percentage appeared larger due to the relatively small Golden value. Assessing the Layer Normalization operator in isolation suggests that using an 8-bit input may pose some risk. However, it is essential to evaluate the impact on the entire model comprehensively to determine its overall effect.

3) *Activation Functions*: Activation functions regulate the transmission of signals between neurons in neural networks, encompassing linear (e.g., $x = f(x)$) and nonlinear functions (e.g., Sigmoid, Tanh, Relu). Nonlinear functions are essential for solving complex problems, as linear functions alone would merely yield a linear combination of the inputs. Consequently, neural networks have adopted nonlinear functions to model and address intricate nonlinear problems more effectively. Various fixed-point representations for activation functions, such as GELU [92], Relu [93], Leaky ReLU [94], ELU [95], SELU [96], Sigmoid [97], and Tanh, have been developed in this study. GELU serves as an illustrative example for discussing the hardware fixed-point design of activation functions.

The original calculation formula for GELU [98] is defined as :

$$GELU(x) = x \cdot \frac{1}{\sqrt{2\pi}} \int_{-\infty}^x e^{-\frac{t^2}{2}} dt \quad (8)$$

$$\simeq x \cdot \text{Sigmoid}(1.702x)$$

Similarly, using the inverse quantization formula, we can transform the GELU calculation into:

$$GELU(x) = \frac{S \cdot (X_Q - zp)}{1 + e^{1.702 \cdot S \cdot (X_Q - zp)}} \quad (9)$$

Following the similar way as that in Softmax, we perform a low-precision replacement for the denominator, changing the base e to base 2, we have:

$$e^{1.702 \cdot S \cdot X_{\Delta_i}} = 2^{1.702 \cdot \log_2^S \cdot S \cdot X_{\Delta_i}}$$

$$\simeq 2^{S \cdot ((X_{\Delta_i} < 1) + (X_{\Delta_i} >> 1) - (X_{\Delta_i} >> 4))}$$

$$= 2^{S \cdot X_p} \quad (10)$$

where:

$$X_p = X_{\Delta_i} + (X_{\Delta_i} >> 1) - (X_{\Delta_i} >> 4) \quad (11)$$

After some derivations, we can obtain the approximate formula for GELU:

$$GELU(x_i) = \frac{S \cdot (X_Q - zp)}{1 + e^{1.702 \cdot S \cdot (X_Q - zp)}} \quad (12)$$

$$= \frac{S \cdot (X_Q - zp) \cdot X_{exp_i}}{X_{exp_i} + X_{exp_{max}}}$$

We developed a fixed-point implementation for the GELU function based on the approximate formula. We tested the implementation using signed $S6.9$ and $S3.4$ for input and signed $S5.10$ and $S3.4$ for output. The test outcomes are displayed in Table III (last three rows). For 16-bit input and output, the average error was below 1%. However, the maximum error was not applicable due to some values near zero. When we changed the input to 8-bit, the average error increased to 5%. Further reducing the output to 8-bit resulted in an average error of approximately 28%, indicating that the output bit width significantly influenced the accuracy of the results.

4) *Matrix Multiplication*: Matrix multiplication constitutes a significant portion of Transformers, accounting for over 80% of their computational load. We analyzed various publicly available perceptual algorithm models and discovered this high proportion [99], [100], [101], [102], [103], [104], [105], [106].

In Transformers, multiply-accumulate operations occur in the channel direction, with each channel requiring completion. Channel lengths can reach up to 256, necessitating consideration of fixed-point calculations and overflow issues during design. Our circuit design accommodates fixed-point arithmetic for INT4, INT8, and INT16, using INT4 multiply-accumulate as the basic unit. By employing shift operations, we utilize 2 INT4 units for INT8 and 4 INT4 units for INT16 implementations. Additionally, we implement FP8, including E4M3 and E5M2 formats for multiply-accumulate operations, using 2 INT4 units and a bypass design. FP8, an IEEE floating-point format, has demonstrated training accuracy comparable to 16-bit precision while offering significant speedups for Transformers and computer vision applications. Intermediate results employ FP16/FP32 or Int32 formats, and partial sums use Float formats combined with scale factors.

Matrix multiplication acceleration requires not only fixed-point design but also precise quantization design. We have made attempts to address this issue by tailoring quantization design to specific data and models, as their corresponding quantization value ranges and scopes differ. This approach helps prevent overflow, which can easily occur due to the large dimensions of multiply-accumulate operations.

5) *Section Summary*: Various optimization techniques were employed to improve Transformer-based models. Data reorganization operators, such as reshape, permute, split, concatenate, and transpose, were used to handle irregular data, relying on on-chip memory for intermediate results storage. Software compiler optimizations, including operator merging and operator mapping, were employed to optimize these operators. Model quantization, a critical technique for accelerating model inference, replaced non-linear operators in Transformer networks with integer polynomial approximation methods or function approximation methods. Alternative quantization methods, such as exponential quantization, were also considered for matrix multiplication acceleration. Model structure improvements, like using efficient attention mechanisms [107], [108] or lightweight structures, contributed to further optimization.

Model compression methods, such as pruning and knowledge distillation, were also investigated. Pruning involved removing unimportant parameters or connections from well-trained models [109], [110], [111], with various approaches focusing on multi-

head self-attention (MHSA), channels, tokens, or entire Transformer structures [112], [113], [114], [115], [116]. Knowledge distillation transferred knowledge from a large teacher model to a smaller student model [117], [118], [119]. Combining model quantization with knowledge distillation reduced memory overhead and enhanced performance [120], [121], [122]. Vision Transformer distillation techniques examined feature maps and attention, with feature map distillation dividing maps into patches and attention distillation using an additional distillation token for knowledge transfer [123], [124], [122].

Research on hardware acceleration for Transformers has primarily focused on NLP models, such as BERT, and vision transformer models, like the ViT. The application of Transformers in the autonomous driving domain rapidly progressed in 2022, which led to increased interest in their implementation. Hardware acceleration for autonomous driving transformer models, however, is still in its infancy. Existing benchmarks from NPU manufacturers reveal the acceleration performance for Swin-transformer and Vision transformer models, but there is limited public information on the acceleration for more recent models such as DETR3D, PETR, and BEVFormer. As Transformer models continue to gain traction in the autonomous driving field, major NPU manufacturers and research institutions are actively exploring acceleration techniques for these models, aiming to deploy them in mass-produced vehicles. In this work, we dissected typical autonomous driving models and developed fixed-point implementations for the resulting operators.

IV. CHALLENGES AND TRENDS

Transformer-based deep learning methods have shown potential for improving autonomous driving systems, but they face challenges such as collecting high-quality training data, ensuring safety, and providing interpretability. Multimodal fusion and explainability are growing trends in the field, while perception and prediction tasks have been successfully accomplished using Transformer-based models. Prospects include optimizing for real-time processing and developing end-to-end learning models. However, addressing the challenges and leveraging the trends and prospects require ongoing research efforts.

Transformer model has evolved from its initial use in 3D obstacle perception tasks to various perception tasks. The future of autonomous driving requires greater system safety and determinism, and single-modal visual perception has reached saturation in terms of marginal gain. Multimodal fusion is required to enhance marginal gain, which is critical for high-level autonomous driving. To meet this demand, larger size, multimodal and multitask Transformer

model with 4D spatio-temporal input/output may be generated in the future. This poses new challenges for model training and acceleration, requiring advances in algorithm design, hardware architecture, and system integration.

Tracking, planning, and decision-making tasks in autonomous driving have also begun to transit from conventional DNN models to Transformer-based models. Given the growing complexity of Transformer models, this may require better hardware acceleration schemes to improve model inference efficiency in hardware deployment. One promising approach is to cascade multiple levels and types of Transformer models into an end-to-end system. However, this presents a challenge in terms of accelerating the entire series of models, as each model may have unique hardware requirements. In the perception-based models, the primary inputs were images or radar data, which were processed through a CNN to extract features. These features were then fed into a BEV perception transformer model for obstacle and static ground marker detection from a BEV perspective. The BEV perception results, combined with high-precision maps, were further encoded into a grid format and input into a NLP-like transformer model to complete the prediction and planning tasks.

In addition to the activation function, LN, Softmax, and large matrix multiplication acceleration of the base model, the Transformer model in autonomous driving tasks has a special Deformable Attention operator. Its learnable position parameters cause some irregularities in the data relevant to each query, which increases the cache pressure on the hardware for image data and makes parallel acceleration difficult. In addition to optimizing software compiler scheduling, hardware needs to be specially designed for such models. Mixed-precision quantization of Transformer models is an important task for accelerating the model, which directly affects computing power and storage and is one of the main research directions in the future. High-bit quantization ensured high precision but required larger memory usage and computational resources, while low-bit quantization offered lower precision but reduced memory and computational demands. Fixed-bit quantization was unable to achieve a fine-grained trade-off between accuracy and computational power, necessitating the use of mixed-precision quantization (MPQ) for efficient model compression. MPQ employed various quantization bit-widths, including 8-bit, 16-bit, 32-bit, and even 4-bit and 2-bit. Besides the mature linear quantization method, alternative approaches, such as logarithmic quantization based on FP8, were considered, with FP8-based quantization and acceleration being a prominent research area.

The attention mechanism of Transformer takes ad-

vantages in converting a spatial sequence into another spatial sequence, as we know that matrix multiply can transform a vector from one space to another space, large matrix can do multidimensional space transformation and parameters in these matrixes are learnable. After space transformation, informations relationship query becomes easier. Then Grid sample in attention can gather features needed from related pixels, and grid sample position is also learnable. Matrix transformation and grid sample makes Transformer well-suited for autonomous driving tasks that require converting multi-view data to BEV format. The parameter and computing power of the Transformer model far exceed those of CNN networks, making it better for generalizing various corner cases and overfitting on large datasets. However, this also increases the complexity of the model and requires careful optimization to ensure efficient performance. Thus, there is a need to develop better interpretable and explainable techniques for Transformer models in autonomous driving, as these are essential for ensuring safety and building trust in the system. For example, attention-based saliency maps could be employed to visually highlight the most important regions in input data, such as camera or LiDAR feeds, that the model uses for making driving decisions. This would provide insights into the model's decision-making process, allowing engineers and users to better understand and trust the system.

V. CONCLUSIONS

This paper presented a comprehensive overview of Transformer-based models tailored specifically for autonomous driving tasks. We examined different architectures for organizing Transformer inputs and outputs and assessed their respective advantages and disadvantages. In-depth exploration of Transformer-related operators and their hardware acceleration analysis was conducted, with considerations of key factors such as quantization and runtime with fixed points. Benchmark comparison was provided for both the tasks and operator level fixed point tests. Lastly, we highlighted the challenges, trends, and current insights in Transformer-based models, discussing their hardware deployment and acceleration issues within the context of longer term Transformer deployment in real world applications.

REFERENCES

- [1] K. Bengler, K. Dietmayer, B. Farber, M. Maurer, C. Stiller, and H. Winner, “Three decades of driver assistance systems: Review and future perspectives,” *IEEE Intelligent transportation systems magazine*, vol. 6, no. 4, pp. 6–22, 2014.
- [2] R. Hussain and S. Zeadally, “Autonomous cars: Research results, issues, and future challenges,” *IEEE Communications Surveys & Tutorials*, vol. 21, no. 2, pp. 1275–1313, 2018.
- [3] S. Grigorescu, B. Trasnea, T. Cocias, and G. Macesanu, “A survey of deep learning techniques for autonomous driving,” *Journal of Field Robotics*, vol. 37, no. 3, pp. 362–386, 2020.
- [4] M. Campbell, M. Egerstedt, J. P. How, and R. M. Murray, “Autonomous driving in urban environments: approaches, lessons and challenges,” *Philosophical Transactions of the Royal Society A: Mathematical, Physical and Engineering Sciences*, vol. 368, no. 1928, pp. 4649–4672, 2010.
- [5] C. Katrakazas, M. Qudus, W.-H. Chen, and L. Deka, “Real-time motion planning methods for autonomous on-road driving: State-of-the-art and future research directions,” *Transportation Research Part C: Emerging Technologies*, vol. 60, pp. 416–442, 2015.
- [6] B. Paden, M. Čáp, S. Z. Yong, D. Yershov, and E. Frazzoli, “A survey of motion planning and control techniques for self-driving urban vehicles,” *IEEE Transactions on intelligent vehicles*, vol. 1, no. 1, pp. 33–55, 2016.
- [7] G. Bresson, Z. Alsayed, L. Yu, and S. Glaser, “Simultaneous localization and mapping: A survey of current trends in autonomous driving,” *IEEE Transactions on Intelligent Vehicles*, vol. 2, no. 3, pp. 194–220, 2017.
- [8] Y. LeCun, Y. Bengio, and G. Hinton, “Deep learning,” *nature*, vol. 521, no. 7553, pp. 436–444, 2015.
- [9] J. Gu, Z. Wang, J. Kuen, L. Ma, A. Shahroudy, B. Shuai, T. Liu, X. Wang, G. Wang, J. Cai *et al.*, “Recent advances in convolutional neural networks,” *Pattern recognition*, vol. 77, pp. 354–377, 2018.
- [10] E. Yurtsever, J. Lambert, A. Carballo, and K. Takeda, “A survey of autonomous driving: Common practices and emerging technologies,” *IEEE access*, vol. 8, pp. 58443–58469, 2020.
- [11] S. Kuutti, R. Bowden, Y. Jin, P. Barber, and S. Fallah, “A survey of deep learning applications to autonomous vehicle control,” *IEEE Transactions on Intelligent Transportation Systems*, vol. 22, no. 2, pp. 712–733, 2020.
- [12] M. R. Bachute and J. M. Subhedar, “Autonomous driving architectures: insights of machine learning and deep learning algorithms,” *Machine Learning with Applications*, vol. 6, p. 100164, 2021.
- [13] D. Parekh, N. Poddar, A. Rajpurkar, M. Chahal, N. Kumar, G. P. Joshi, and W. Cho, “A review on autonomous vehicles: Progress, methods and challenges,” *Electronics*, vol. 11, no. 14, p. 2162, 2022.
- [14] B. R. Kiran, I. Sobh, V. Talpaert, P. Mannion, A. A. Al Sallab, S. Yogamani, and P. Pérez, “Deep reinforcement learning for autonomous driving: A survey,” *IEEE Transactions on Intelligent Transportation Systems*, vol. 23, no. 6, pp. 4909–4926, 2021.
- [15] S. Y. Alaba and J. E. Ball, “Deep learning-based image 3d object detection for autonomous driving,” *IEEE Sensors Journal*, 2023.
- [16] S. Mozaffari, O. Y. Al-Jarrah, M. Dianati, P. Jennings, and A. Mouzakitis, “Deep learning-based vehicle behavior prediction for autonomous driving applications: A review,” *IEEE Transactions on Intelligent Transportation Systems*, vol. 23, no. 1, pp. 33–47, 2020.
- [17] Y. Huang, J. Du, Z. Yang, Z. Zhou, L. Zhang, and H. Chen, “A survey on trajectory-prediction methods for autonomous driving,” *IEEE Transactions on Intelligent Vehicles*, vol. 7, no. 3, pp. 652–674, 2022.
- [18] Y. Cui, R. Chen, W. Chu, L. Chen, D. Tian, Y. Li, and D. Cao, “Deep learning for image and point cloud fusion in autonomous driving: A review,” *IEEE Transactions on Intelligent Transportation Systems*, vol. 23, no. 2, pp. 722–739, 2021.
- [19] W. Schwarting, J. Alonso-Mora, and D. Rus, “Planning and decision-making for autonomous vehicles,” *Annual Review of Control, Robotics, and Autonomous Systems*, vol. 1, pp. 187–210, 2018.
- [20] Q. Liu, X. Li, S. Yuan, and Z. Li, “Decision-making technology for autonomous vehicles: Learning-based methods, applications and future outlook,” in *2021 IEEE International Intelligent Transportation Systems Conference (ITSC)*. IEEE, 2021, pp. 30–37.
- [21] S. Abdallaoui, E.-H. Aglzim, A. Chaibet, and A. Kribèche, “Thorough review analysis of safe control of autonomous vehicles: path planning and navigation techniques,” *Energies*, vol. 15, no. 4, p. 1358, 2022.
- [22] É. Zablocki, H. Ben-Younes, P. Pérez, and M. Cord, “Explainability of deep vision-based autonomous driving systems: Review and challenges,” *International Journal of Computer Vision (IJCV 2022)*, vol. 130, no. 10, pp. 2425–2452, 2022.
- [23] W. Ding, C. Xu, M. Arief, H. Lin, B. Li, and D. Zhao, “A survey on safety-critical driving scenario generation—a methodological perspective,” *IEEE Transactions on Intelligent Transportation Systems*, 2023.
- [24] A. Vaswani, N. Shazeer, N. Parmar, J. Uszkoreit, L. Jones, A. N. Gomez, Ł. Kaiser, and I. Polosukhin, “Attention is all you need,” *31st Conference on Neural Information Processing Systems (NIPS 2017)*, vol. 30, 2017.
- [25] D. Bahdanau, K. H. Cho, and Y. Bengio, “Neural machine translation by jointly learning to align and translate,” in *3rd International Conference on Learning Representations (ICLR)*, 2015.
- [26] M.-T. Luong, H. Pham, and C. D. Manning, “Effective approaches to attention-based neural machine translation,” in *The 2015 Conference on Empirical Methods in Natural Language Processing*, 2015, pp. 1412–1421.
- [27] J. Devlin, M.-W. Chang, K. Lee, and K. Toutanova, “Bert: Pre-training of deep bidirectional transformers for language understanding,” in *The 17th Annual Conference of the North American Chapter of the Association for Computational Linguistics: Human Language Technologies (NAACL-HLT 2019)*, 2019, pp. 4171–4186.
- [28] A. Radford, K. Narasimhan, T. Salimans, and I. Sutskever, “Improving language understanding by generative pre-training,” 2018.
- [29] A. Dosovitskiy, L. Beyer, A. Kolesnikov, D. Weissenborn, X. Zhai, T. Unterthiner, M. Dehghani, M. Minderer, G. Heigold, S. Gelly, J. Uszkoreit, and N. Houlsby, “An image is worth 16x16 words: Transformers for image recognition at scale,” *ICLR*, 2021.
- [30] Z. Liu, Y. Lin, Y. Cao, H. Hu, Y. Wei, Z. Zhang, S. Lin, and B. Guo, “Swin transformer: Hierarchical vision transformer using shifted windows,” in *Proceedings of the IEEE/CVF international conference on computer vision (ICCV)*, 2021, pp. 10012–10022.
- [31] Z. Liu, H. Tang, A. Amini, X. Yang, H. Mao, D. Rus, and S. Han, “Bevfusion: Multi-task multi-sensor fusion with unified bird’s-eye view representation,” 2023.
- [32] T. Liang, H. Xie, K. Yu, Z. Xia, Z. Lin, Y. Wang, T. Tang, B. Wang, and Z. Tang, “BEVFusion: A Simple and Robust LiDAR-Camera Fusion Framework,” in *Neural Information Processing Systems (NeurIPS)*, 2022.
- [33] Y. Zhang, Z. Zhu, W. Zheng, J. Huang, G. Huang, J. Zhou, and J. Lu, “Beverse: Unified perception and prediction in birds-eye-view for vision-centric autonomous driving,” *arXiv preprint arXiv:2205.09743*, 2022.
- [34] Y. Wang, V. C. Guizilini, T. Zhang, Y. Wang, H. Zhao, and J. Solomon, “Det3d: 3d object detection from multi-view images via 3d-to-2d queries,” in *Conference on Robot Learning*, 2021, pp. 180–191.
- [35] X. Chen, T. Zhang, Y. Wang, Y. Wang, and H. Zhao, “Futr3d: A unified sensor fusion framework for 3d detection,” *arXiv preprint arXiv:2203.10642*, 2022.
- [36] Y. Liu, T. Wang, X. Zhang, and J. Sun, “Pet: Position embedding transformation for multi-view 3d object detection,” in *Computer Vision—ECCV 2022: 17th European Confer-*

- ence, Tel Aviv, Israel, October 23–27, 2022, *Proceedings, Part XXVII*. Springer, 2022, pp. 531–548.
- [37] Y. Liu, J. Yan, F. Jia, S. Li, Q. Gao, T. Wang, X. Zhang, and J. Sun, “PetrV2: A unified framework for 3d perception from multi-camera images,” *arXiv preprint arXiv:2206.01256*, 2022.
- [38] C.-Y. Tseng, Y.-R. Chen, H.-Y. Lee, T.-H. Wu, W.-C. Chen, and W. Hsu, “Crossdr: Cross-view and depth-guided transformers for 3d object detection,” *The 40th IEEE International Conference on Robotics and Automation (ICRA 2023)*, 2023.
- [39] Z. Li, W. Wang, H. Li, E. Xie, C. Sima, T. Lu, Y. Qiao, and J. Dai, “Befvformer: Learning bird’s-eye-view representation from multi-camera images via spatiotemporal transformers,” in *Computer Vision–ECCV 2022: 17th European Conference, Tel Aviv, Israel, October 23–27, 2022, Proceedings, Part IX*. Springer, 2022, pp. 1–18.
- [40] C. Yang, Y. Chen, H. Tian, C. Tao, X. Zhu, Z. Zhang, G. Huang, H. Li, Y. Qiao, L. Lu *et al.*, “Befvformer v2: Adapting modern image backbones to bird’s-eye-view recognition via perspective supervision,” *arXiv preprint arXiv:2211.10439*, 2022.
- [41] Y. Li, Y. Chen, X. Qi, Z. Li, J. Sun, and J. Jia, “Unifying voxel-based representation with transformer for 3d object detection,” in *36th Conference on Neural Information Processing Systems (NeurIPS 2022)*, 2022.
- [42] Y. Huang, W. Zheng, Y. Zhang, J. Zhou, and J. Lu, “Tri-perspective view for vision-based 3d semantic occupancy prediction,” *Proceedings of the IEEE/CVF Conference on Computer Vision and Pattern Recognition*, 2023.
- [43] Y. Li, Z. Yu, C. Choy, C. Xiao, J. M. Alvarez, S. Fidler, C. Feng, and A. Anandkumar, “Voxformer: Sparse voxel transformer for camera-based 3d semantic scene completion,” in *The IEEE / CVF Computer Vision and Pattern Recognition Conference (CVPR)*, 2023.
- [44] Y. Wei, L. Zhao, W. Zheng, Z. Zhu, J. Zhou, and J. Lu, “Surroundocc: Multi-camera 3d occupancy prediction for autonomous driving,” in *The IEEE / CVF Computer Vision and Pattern Recognition Conference (CVPR)*, 2023.
- [45] F. Zeng, B. Dong, Y. Zhang, T. Wang, X. Zhang, and Y. Wei, “Motr: End-to-end multiple-object tracking with transformer,” in *Computer Vision–ECCV 2022: 17th European Conference, Tel Aviv, Israel, October 23–27, 2022, Proceedings, Part XXVII*. Springer, 2022, pp. 659–675.
- [46] T. Zhang, X. Chen, Y. Wang, Y. Wang, and H. Zhao, “Mutr3d: A multi-camera tracking framework via 3d-to-2d queries,” in *Proceedings of the IEEE/CVF Conference on Computer Vision and Pattern Recognition*, 2022, pp. 4537–4546.
- [47] L. Peng, Z. Chen, Z. Fu, P. Liang, and E. Cheng, “Bevsegformer: Bird’s eye view semantic segmentation from arbitrary camera rigs,” in *Proceedings of the IEEE/CVF Winter Conference on Applications of Computer Vision*, 2023, pp. 5935–5943.
- [48] L. Chen, C. Sima, Y. Li, Z. Zheng, J. Xu, X. Geng, H. Li, C. He, J. Shi, Y. Qiao, and J. Yan, “Persformer: 3d lane detection via perspective transformer and the openlane benchmark,” in *European Conference on Computer Vision (ECCV)*, 2022.
- [49] R. Liu, Z. Yuan, T. Liu, and Z. Xiong, “End-to-end lane shape prediction with transformers,” in *Proceedings of the IEEE/CVF winter conference on applications of computer vision*, 2021, pp. 3694–3702.
- [50] Y. Bai, Z. Chen, Z. Fu, L. Peng, P. Liang, and E. Cheng, “Curveformer: 3d lane detection by curve propagation with curve queries and attention,” *IEEE Conference on Robotics and Automation, ICRA 2023*, 2023.
- [51] A. Saha, O. Mendez, C. Russell, and R. Bowden, “Translating images into maps,” in *2022 International Conference on Robotics and Automation (ICRA)*. IEEE, 2022, pp. 9200–9206.
- [52] Z. Li, W. Wang, E. Xie, Z. Yu, A. Anandkumar, J. M. Alvarez, P. Luo, and T. Lu, “Panoptic segformer: Delving deeper into panoptic segmentation with transformers,” in *Proceedings of the IEEE/CVF Conference on Computer Vision and Pattern Recognition*, 2022, pp. 1280–1289.
- [53] Y. B. Can, A. Liniger, D. P. Paudel, and L. Van Gool, “Structured bird’s-eye-view traffic scene understanding from on-board images,” in *Proceedings of the IEEE/CVF international conference on computer vision (ICCV)*, 2021, pp. 15 661–15 670.
- [54] Y. Liu, Y. Wang, Y. Wang, and H. Zhao, “Vectormapnet: End-to-end vectorized hd map learning,” *arXiv preprint arXiv:2206.08920*, 2022.
- [55] B. Liao, S. Chen, X. Wang, T. Cheng, Q. Zhang, W. Liu, and C. Huang, “Maptr: Structured modeling and learning for online vectorized hd map construction,” in *International Conference on Learning Representations*, 2023.
- [56] J. Gao, C. Sun, H. Zhao, Y. Shen, D. Anguelov, C. Li, and C. Schmid, “Vectormet: Encoding hd maps and agent dynamics from vectorized representation,” in *Proceedings of the IEEE/CVF Conference on Computer Vision and Pattern Recognition*, 2020, pp. 11 525–11 533.
- [57] J. Gu, C. Sun, and H. Zhao, “Densetnt: End-to-end trajectory prediction from dense goal sets,” in *Proceedings of the IEEE/CVF international conference on computer vision (ICCV)*, 2021, pp. 15 303–15 312.
- [58] Y. Liu, J. Zhang, L. Fang, Q. Jiang, and B. Zhou, “Multimodal motion prediction with stacked transformers,” in *Proceedings of the IEEE/CVF Conference on Computer Vision and Pattern Recognition*, 2021, pp. 7577–7586.
- [59] Y. Yuan, X. Weng, Y. Ou, and K. M. Kitani, “Agentformer: Agent-aware transformers for socio-temporal multi-agent forecasting,” in *Proceedings of the IEEE/CVF International Conference on Computer Vision (ICCV)*, 2021, pp. 9813–9823.
- [60] N. Nayakanti, R. Al-Rfou, A. Zhou, K. Goel, K. S. Refaat, and B. Sapp, “Wayformer: Motion forecasting via simple & efficient attention networks,” *arXiv preprint arXiv:2207.05844*, 2022.
- [61] K. Chitta, A. Prakash, B. Jaeger, Z. Yu, K. Renz, and A. Geiger, “Transfuser: Imitation with transformer-based sensor fusion for autonomous driving,” *IEEE Transactions on Pattern Analysis and Machine Intelligence*, 2022.
- [62] K. Chitta, A. Prakash, and A. Geiger, “Neat: Neural attention fields for end-to-end autonomous driving,” in *Proceedings of the IEEE/CVF international conference on computer vision (ICCV)*, 2021.
- [63] H. Shao, L. Wang, R. Chen, H. Li, and Y. Liu, “Safety-enhanced autonomous driving using interpretable sensor fusion transformer,” in *6th Conference on Robot Learning (CoRL 2022)*. PMLR, 2022, pp. 726–737.
- [64] Q. Zhang, M. Tang, R. Geng, F. Chen, R. Xin, and L. Wang, “Mmfn: Multi-modal-fusion-net for end-to-end driving,” in *2022 IEEE/RSJ International Conference on Intelligent Robots and Systems (IROS)*. IEEE, 2022, pp. 8638–8643.
- [65] S. Hu, L. Chen, P. Wu, H. Li, J. Yan, and D. Tao, “Step3: End-to-end vision-based autonomous driving via spatial-temporal feature learning,” in *Computer Vision–ECCV 2022: 17th European Conference, Tel Aviv, Israel, October 23–27, 2022, Proceedings, Part XXXVIII*. Springer, 2022, pp. 533–549.
- [66] Y. Hu, J. Yang, L. Chen, K. Li, C. Sima, X. Zhu, S. Chai, S. Du, T. Lin, W. Wang, L. Lu, X. Jia, Q. Liu, J. Dai, Y. Qiao, and H. Li, “Planning-oriented autonomous driving,” 2023.
- [67] N. Carion, F. Massa, G. Synnaeve, N. Usunier, A. Kirillov, and S. Zagoruyko, “End-to-end object detection with transformers,” in *Computer Vision–ECCV 2020: 16th European Conference, Glasgow, UK, August 23–28, 2020, Proceedings, Part I 16*. Springer, 2020, pp. 213–229.
- [68] X. Zhu, W. Su, L. Lu, B. Li, X. Wang, and J. Dai, “Deformable detr: Deformable transformers for end-to-end object detection,” *Ninth International Conference on Learning Representations (ICLR 2021)*, 2020.
- [69] D. Gong, J. Lee, M. Kim, S. J. Ha, and M. Cho, “Future transformer for long-term action anticipation,” in *The IEEE / CVF Computer Vision and Pattern Recognition Conference (CVPR)*, 2022, pp. 3052–3061.

- [70] Q. Li, Y. Wang, Y. Wang, and H. Zhao, "Hdmapnet: An online hd map construction and evaluation framework," in *2022 International Conference on Robotics and Automation (ICRA)*. IEEE, 2022, pp. 4628–4634.
- [71] J. Deng, W. Dong, R. Socher, L.-J. Li, K. Li, and L. Fei-Fei, "Imagenet: A large-scale hierarchical image database," in *2009 IEEE conference on computer vision and pattern recognition*. Ieee, 2009, pp. 248–255.
- [72] T.-Y. Lin, M. Maire, S. Belongie, J. Hays, P. Perona, D. Ramanan, P. Dollár, and C. L. Zitnick, "Microsoft coco: Common objects in context," in *Computer Vision—ECCV 2014: 13th European Conference, Zurich, Switzerland, September 6–12, 2014, Proceedings, Part V 13*. Springer, 2014, pp. 740–755.
- [73] H. Caesar, V. Bankiti, A. H. Lang, S. Vora, V. E. Liong, Q. Xu, A. Krishnan, Y. Pan, G. Baldan, and O. Beijbom, "nusscenes: A multimodal dataset for autonomous driving," in *Proceedings of the IEEE/CVF conference on computer vision and pattern recognition*, 2020, pp. 11 621–11 631.
- [74] S. Yoo, H. S. Lee, H. Myeong, S. Yun, H. Park, J. Cho, and D. H. Kim, "End-to-end lane marker detection via row-wise classification," in *Proceedings of the IEEE/CVF Conference on Computer Vision and Pattern Recognition Workshops*, 2020, pp. 1006–1007.
- [75] L. Chen, C. Sima, Y. Li, Z. Zheng, J. Xu, X. Geng, H. Li, C. He, J. Shi, Y. Qiao, and J. Yan, "Persformer: 3d lane detection via perspective transformer and the openlane benchmark," in *European Conference on Computer Vision (ECCV)*, 2022.
- [76] M.-F. Chang, J. Lambert, P. Sangkloy, J. Singh, S. Bak, A. Hartnett, D. Wang, P. Carr, S. Lucey, D. Ramanan *et al.*, "Argoverse: 3d tracking and forecasting with rich maps," in *Proceedings of the IEEE/CVF conference on computer vision and pattern recognition*, 2019, pp. 8748–8757.
- [77] A. Dosovitskiy, G. Ros, F. Codevilla, A. Lopez, and V. Koltun, "Carla: An open urban driving simulator," in *Conference on robot learning*. PMLR, 2017, pp. 1–16.
- [78] H. Zhao, J. Gao, T. Lan, C. Sun, B. Sapp, B. Varadarajan, Y. Shen, Y. Shen, Y. Chai, C. Schmid *et al.*, "Tnt: Target-driven trajectory prediction," in *Conference on Robot Learning*. PMLR, 2021, pp. 895–904.
- [79] J. Dai, H. Qi, Y. Xiong, Y. Li, G. Zhang, H. Hu, and Y. Wei, "Deformable convolutional networks," in *2017 IEEE International Conference on Computer Vision (ICCV)*, 2017, pp. 764–773.
- [80] K. He, X. Zhang, S. Ren, and J. Sun, "Deep residual learning for image recognition," in *Proceedings of the IEEE conference on computer vision and pattern recognition*, 2016, pp. 770–778.
- [81] Z. Liu, Y. Wang, K. Han, W. Zhang, S. Ma, and W. Gao, "Post-training quantization for vision transformer," *35th Conference on Neural Information Processing Systems (NeurIPS 2021)*, vol. 34, pp. 28 092–28 103, 2021.
- [82] H. Bai, L. Hou, L. Shang, X. Jiang, I. King, and M. R. Lyu, "Towards efficient post-training quantization of pre-trained language models," *36th Conference on Neural Information Processing Systems*, vol. 35, pp. 1405–1418, 2022.
- [83] S. Kim, A. Gholami, Z. Yao, M. W. Mahoney, and K. Keutzer, "I-bert: Integer-only bert quantization," in *International conference on machine learning*. PMLR, 2021, pp. 5506–5518.
- [84] D. Zhu, S. Lu, M. Wang, J. Lin, and Z. Wang, "Efficient precision-adjustable architecture for softmax function in deep learning," *IEEE Transactions on Circuits and Systems II: Express Briefs*, vol. 67, no. 12, pp. 3382–3386, 2020.
- [85] Y. Gao, W. Liu, and F. Lombardi, "Design and implementation of an approximate softmax layer for deep neural networks," in *2020 IEEE International Symposium on Circuits and Systems (ISCAS)*. IEEE, 2020, pp. 1–5.
- [86] G. Du, C. Tian, Z. Li, D. Zhang, Y. Yin, and Y. Ouyang, "Efficient softmax hardware architecture for deep neural networks," in *Proceedings of the 2019 on Great Lakes Symposium on VLSI*, 2019, pp. 75–80.
- [87] J. R. Stevens, R. Venkatesan, S. Dai, B. Khailany, and A. Raghunathan, "Softermax: Hardware/software co-design of an efficient softmax for transformers," in *2021 58th ACM/IEEE Design Automation Conference (DAC)*. IEEE, 2021, pp. 469–474.
- [88] J. L. Ba, J. R. Kiros, and G. E. Hinton, "Layer normalization," *arXiv preprint arXiv:1607.06450*, 2016.
- [89] E. Hoffer, R. Banner, I. Golan, and D. Soudry, "Norm matters: efficient and accurate normalization schemes in deep networks," *32nd Conference on Neural Information Processing Systems (NeurIPS 2018)*, vol. 31, 2018.
- [90] Y. Lin, Y. Li, T. Liu, T. Xiao, T. Liu, and J. Zhu, "Towards fully 8-bit integer inference for the transformer model," *the 29th International Joint Conference on Artificial Intelligence and the 17th Pacific Rim International Conference on Artificial Intelligence (IJCAI-PRICAI2020)*, 2020.
- [91] Y. Lin, T. Zhang, P. Sun, Z. Li, and S. Zhou, "Fq-vit: Post-training quantization for fully quantized vision transformer," in *Proceedings of the Thirty-First International Joint Conference on Artificial Intelligence, IJCAI-22*, 2022, pp. 1173–1179.
- [92] D. Hendrycks and K. Gimpel, "Gaussian error linear units (gelus)," *arXiv preprint arXiv:1606.08415*, 2016.
- [93] X. Glorot, A. Bordes, and Y. Bengio, "Deep sparse rectifier neural networks," in *Proceedings of the fourteenth international conference on artificial intelligence and statistics. JMLR Workshop and Conference Proceedings*, 2011, pp. 315–323.
- [94] A. L. Maas, A. Y. Hannun, A. Y. Ng *et al.*, "Rectifier nonlinearities improve neural network acoustic models," in *Proc. icml*, vol. 30, no. 1. Atlanta, Georgia, USA, 2013, p. 3.
- [95] D.-A. Clevert, T. Unterthiner, and S. Hochreiter, "Fast and accurate deep network learning by exponential linear units (elus)," *4th International Conference on Learning Representations, ICLR 2016*, 2016.
- [96] G. Klambauer, T. Unterthiner, A. Mayr, and S. Hochreiter, "Self-normalizing neural networks," *31st Conference on Neural Information Processing Systems (NIPS 2017)*, vol. 30, 2017.
- [97] J. Mount, "The equivalence of logistic regression and maximum entropy models," URL: <http://www.win-vector.com/dfiles/LogisticRegressionMaxEnt.pdf>, 2011.
- [98] Q. G. Zhikai Li, "I-vit: Integer-only quantization for efficient vision transformer inference," *arXiv preprint arXiv:2207.01405*, 2022.
- [99] N. Wang, J. Choi, D. Brand, C.-Y. Chen, and K. Gopalakrishnan, "Training deep neural networks with 8-bit floating point numbers," *32nd Conference on Neural Information Processing Systems (NeurIPS 2018)*, vol. 31, 2018.
- [100] X. Sun, J. Choi, C.-Y. Chen, N. Wang, S. Venkataramani, V. V. Srinivasan, X. Cui, W. Zhang, and K. Gopalakrishnan, "Hybrid 8-bit floating point (hfp8) training and inference for deep neural networks," *33rd Conference on Neural Information Processing Systems (NeurIPS 2019)*, vol. 32, 2019.
- [101] S. Venkataramani, V. Srinivasan, W. Wang, S. Sen, J. Zhang, A. Agrawal, M. Kar, S. Jain, A. Mannari, H. Tran *et al.*, "Rapid: Ai accelerator for ultra-low precision training and inference," in *2021 ACM/IEEE 48th Annual International Symposium on Computer Architecture (ISCA)*. IEEE, 2021, pp. 153–166.
- [102] "Nvidia, arm, and intel publish fp8 specification for standardization as an interchange format for ai," shorturl.at/bkCPS, accessed: 2023-04-07.
- [103] A. Agrawal, S. K. Lee, J. Silberman, M. Ziegler, M. Kang, S. Venkataramani, N. Cao, B. Fleischer, M. Guillorn, M. Cohen *et al.*, "9.1 a 7nm 4-core ai chip with 25.6 tflops hybrid fp8 training, 102.4 tops int4 inference and workload-aware throttling," in *2021 IEEE International Solid-State Circuits Conference (ISSCC)*, vol. 64. IEEE, 2021, pp. 144–146.
- [104] A. Bhandare, V. Sripathi, D. Karkada, V. Menon, S. Choi, K. Datta, and V. Saletore, "Efficient 8-bit quantization of transformer neural machine language translation model," *36th International Conference on Machine Learning*, 2019.
- [105] M. Nagel, M. v. Baalen, T. Blankevoort, and M. Welling, "Data-free quantization through weight equalization and

- bias correction,” in *Proceedings of the IEEE/CVF International Conference on Computer Vision*, 2019, pp. 1325–1334.
- [106] O. Zafrir, G. Boudoukh, P. Izsak, and M. Wasserblat, “Q8bert: Quantized 8bit bert,” in *2019 Fifth Workshop on Energy Efficient Machine Learning and Cognitive Computing-NeurIPS Edition (EMC2-NIPS)*. IEEE, 2019, pp. 36–39.
- [107] P. Michel, O. Levy, and G. Neubig, “Are sixteen heads really better than one?” *33rd Conference on Neural Information Processing Systems (NeurIPS 2019)*, vol. 32, 2019.
- [108] A. J. Angela Fan, Edouard Grave, “Reducing transformer depth on demand with structured dropout,” *Eighth International Conference on Learning Representations (ICLR 2020)*, 2019.
- [109] N. A. Mitchell A. Gordon, Kevin Duh, “Compressing bert: studying the effects of weight pruning on transfer learning,” *Proceedings of the 5th Workshop on Representation Learning for NLP*, 2020.
- [110] Z. T. Wenxuan Wang, “Rethinking the value of transformer components,” *The 28th International Conference on Computational Linguistics (COLING 2020)*, 2020.
- [111] J. McCarley, R. Chakravarti, and A. Sil, “Structured pruning of a bert-based question answering model,” *arXiv preprint arXiv:1910.06360*, 2019.
- [112] H. He, J. Liu, Z. Pan, J. Cai, J. Zhang, D. Tao, and B. Zhuang, “Pruning self-attentions into convolutional layers in single path,” *The IEEE / CVF Computer Vision and Pattern Recognition Conference (CVPR)*, 2021.
- [113] K. H. Mingjian Zhu, Yehui Tang, “Vision transformer pruning,” *The IEEE / CVF Computer Vision and Pattern Recognition Conference (CVPR)*, 2021.
- [114] S. Kim, S. Shen, D. Thorsley, A. Gholami, W. Kwon, J. Hassoun, and K. Keutzer, “Learned token pruning for transformers,” in *Proceedings of the 28th ACM SIGKDD Conference on Knowledge Discovery and Data Mining*, 2022, pp. 784–794.
- [115] J. W. Hao Yu, “A unified pruning framework for vision transformers,” *The IEEE / CVF Computer Vision and Pattern Recognition Conference (CVPR)*, 2021.
- [116] H. Yang, H. Yin, M. Shen, P. Molchanov, H. Li, and J. Kautz, “Global vision transformer pruning with hessian-aware saliency,” in *The IEEE / CVF Computer Vision and Pattern Recognition Conference (CVPR)*, 2021.
- [117] V. Sanh, L. Debut, J. Chaumond, and T. Wolf, “Distilbert, a distilled version of bert: smaller, faster, cheaper and lighter,” *33rd Conference on Neural Information Processing Systems*, 2019.
- [118] S. Sun, Y. Cheng, Z. Gan, and J. Liu, “Patient knowledge distillation for bert model compression,” *2019 Conference on Empirical Methods in Natural Language Processing and 9th International Joint Conference on Natural Language Processing (EMNLP-IJCNLP 2019)*, 2019.
- [119] X. Jiao, Y. Yin, L. Shang, X. Jiang, X. Chen, L. Li, F. Wang, and Q. Liu, “Tinybert: Distilling bert for natural language understanding,” *The 2020 Conference on Empirical Methods in Natural Language Processing (EMNLP 2020)*, 2020.
- [120] W. Zhang, L. Hou, Y. Yin, L. Shang, X. Chen, X. Jiang, and Q. Liu, “Ternarybert: Distillation-aware ultra-low bit bert,” *The 2020 Conference on Empirical Methods in Natural Language Processing (EMNLP 2020)*, 2020.
- [121] H. Bai, W. Zhang, L. Hou, L. Shang, J. Jin, X. Jiang, Q. Liu, M. Lyu, and I. King, “Binarybert: Pushing the limit of bert quantization,” *Proceedings of the 59th Annual Meeting of the Association for Computational Linguistics and the 11th International Joint Conference on Natural Language Processing*, 2020.
- [122] H. Touvron, M. Cord, M. Douze, F. Massa, A. Sablayrolles, and H. Jégou, “Training data-efficient image transformers & distillation through attention,” in *Proceedings of the 38th International Conference on Machine Learning*. PMLR, 2021, pp. 10 347–10 357.
- [123] S. Lin, H. Xie, B. Wang, K. Yu, X. Chang, X. Liang, and G. Wang, “Knowledge distillation via the target-aware transformer,” in *Proceedings of the IEEE/CVF Conference on Computer Vision and Pattern Recognition*, 2022, pp. 10915–10924.
- [124] R. Liu, K. Yang, A. Roitberg, J. Zhang, K. Peng, H. Liu, and R. Stiefelhagen, “Transkd: Transformer knowledge distillation for efficient semantic segmentation,” in *The IEEE / CVF Computer Vision and Pattern Recognition Conference (CVPR)*, 2022.